

CONTRAST ENHANCEMENT OF MICROSCOPIC MALARIA IMAGES USING MODIFIED LINEAR CONTRAST STRETCHING WITH COLOR PRESERVING FRAMEWORK

DONI SETYAWAN¹, RETANTYO WARDOYO^{2,*}, MOH EDI WIBOWO²
AND ELSA HERDIANA MURHANDARWATI³

¹Doctoral Program, Department of Computer Science and Electronics

²Department of Computer Science and Electronics

³Department of Parasitology

Universitas Gadjah Mada

Bulak Sumur, Yogyakarta 55281, Indonesia

doniset@mail.ugm.ac.id; {mediw; elsa.herdiana}@ugm.ac.id

*Corresponding author: rw@ugm.ac.id

Received September 2022; accepted December 2022

ABSTRACT. *The digital image acquisition of blood smears using a microscope may result in low-contrast images. Low contrast images make identifying Plasmodium-infected cells difficult, which can lead to false diagnoses. Several methods of contrast improvement in malaria images can cause color changes in the processed image. In this paper, we proposed an improved method to enhance the contrast of color malaria images while retaining the coloring structure of the original image. The proposed method used the average value of local and global features to reduce the total dependency on each color component. Furthermore, the color preservation framework was used to improve the maintenance of color information. Based on the experimental results using the MP-IDB dataset, the proposed IMLCS-CPF method gave the best PNSR and AMBE values compared to LCS, MLCS, and IMLCS methods. Visually, the proposed method provided better contrast enhancement while preserving the color information of the original image, thus clarifying the appearance of Plasmodium and erythrocytes in the image of thin blood smears. The enhanced images are expected to help improve the performance of visual examination of malaria through a microscope or facilitate the segmentation process in an automatic malaria diagnosis system.*

Keywords: Malaria, Plasmodium, Contrast enhancement, Color preservation

1. **Introduction.** Malaria is an infectious disease caused by Plasmodium parasites and transmitted by female Anopheles mosquitoes in countries with tropical and subtropical climates [1]. Headaches, fever, and fatigue are typical symptoms of malaria, but in severe cases, malaria can cause seizures and coma, leading to death [2]. According to the World Health Organization (WHO), in 2020, there were an estimated 241 million malaria cases in 85 countries with malaria endemicity, up from 227 million cases in 2019, with the majority of this rise coming from the African Region [3]. Plasmodium parasites that cause malaria in humans are Plasmodium vivax, Plasmodium falciparum, Plasmodium malariae, Plasmodium ovale, and Plasmodium knowlesi. During the infection phase in peripheral blood, each of these plasmodia goes through four life-cycle stages: ring, trophozoite, schizont, and gametocyte [4].

The gold-standard malaria diagnosis is based on a visual microscopic examination of thick and thin blood smears [5]. The advantages of using a microscope are that it can detect all Plasmodium species, calculate the level of parasitemia, observe drug resistance, and lower cost than other techniques. However, the primary drawbacks of this method

are the extensive training needed for a microscopist to read malaria slides proficiently, the high costs associated with training and employing, maintaining skills, and the significant amount of manual labor required. These problems have encouraged attempts to perform the diagnosis of malaria automatically. Automatic malaria diagnosis has several advantages: it gives blood film interpretation that is more reliable and consistent, allows more patients to be handled, and reduces diagnostics costs [2]. Automatic malaria diagnosis consists of five primary steps: image acquisition, preprocessing, segmentation, feature extraction, and classification [6,7]. The digital image acquisition of blood smears using a microscope may result in low-contrast images because of the lack of lighting. Low contrast images make identifying Plasmodium-infected cells difficult, which can lead to false diagnoses [8]. Therefore, contrast enhancement is required at the preprocessing stage to improve the quality of an image [9].

Various contrast enhancement methods have been developed and applied to malaria images. The local histogram equalization [10] and gamma equalization [11,12] were used to enhance the visibility of red blood cells (RBC) and parasites on grayscale microscopic malaria images. Histogram equalization (HE) works by remapping the pixel intensity in the image using a probability distribution [13]. The use of HE can increase the contrast, but the mean brightness of the resulting image becomes in the middle of the gray level range [14]. In gamma equalization, to get the best contrast, it is necessary to experiment on several images to obtain the optimal gamma value. In addition to grayscale images, contrast enhancement methods were also used on the green channel of malaria images, such as Contrast Limited Adaptive Histogram Equalization (CLAHE) [15] and adaptive histogram equalization [16]. Contrast improvement in malaria images has also been carried out on color images which consist of red, green, and blue (RGB) channels. Some approaches that have been used include modified global contrast stretching (MGCS) [17,18], modified linear contrast stretching (MLCS) [19], power law transformation [20], and histogram matching [21]. Compared to MGCS, the contrast resulting from MLCS is better, but there is a color difference in the MLCS image with the input image because the enhancement process is based on the local values of each channel. Power law transformation has the same problem as gamma equalization. It takes some experiments that can be affected by the image used. In histogram matching, the resulting contrast depends on the image used as a reference.

In actual malaria diagnosis, the examination is carried out through color images. Therefore, contrast enhancement on the RGB malaria images becomes essential. In this study, we propose an improvement to the MLCS to increase the contrast of color malaria images while retaining the coloring structure of the original image. The contributions of the paper are 1) the contrast enhancement of malaria images using improved MLCS (IMLCS) by reducing dependence on the local features of each channel to minimize color changes in the resulting image, 2) the use of the color-preserving framework for color restoration [22], the color preservation framework can maintain color information from the input image so that it can be used to overcome the problem of changing the coloration of the contrast-enhanced image, and 3) analyzing the performance comparison of IMLCS with the color preservation framework (IMLCS-CPF) with LCS, MLCS, and IMLCS methods. The proposed IMLCS-CPF method is expected to improve the performance of visual examination of malaria through a microscope or facilitate the segmentation process in an automatic malaria diagnosis system.

The rest of this work is organized as follows. Section 2 describes the proposed method in detail. Section 3 shows the dataset description and discussion of the experimental results. Finally, Section 4 concludes the proposed work.

2. Proposed Method. The proposed method was implemented in two main steps: 1) contrast enhancement of colored malarial microscopic raw images using improved MLCS;

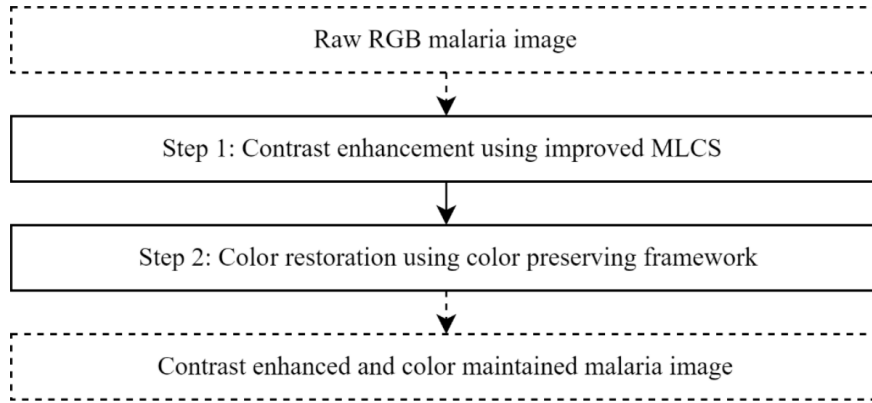


FIGURE 1. Flow chart of the proposed method

2) color restoration to maintain the color structure of the input image using the color preserving framework. The flow chart of the proposed method is shown in Figure 1.

The detailed steps of the proposed method in Figure 1 are described as follows.

Step 0: The input image $f_{RGB}(x, y)$ is a low contrast malaria image. $f_R(x, y)$, $f_G(x, y)$, $f_B(x, y)$ are the red, green, and blue components of $f_{RGB}(x, y)$, respectively.

Step 1: In this step, contrast enhancement was performed using improved MLCS based on the original MLCS in [19]. In the original MLCS, the determination of the minimum and maximum values depends entirely on the local features of each color component. This total dependency can result in a different coloring structure between the input and output image resulting from the enhancement process. Therefore, in improved MLCS, the dependence on local features is reduced to minimize color changes in the image resulting from the enhancement process. The dependency on local features is reduced by calculating the average value obtained from the sum of local features for each color component and global features for all color components. The procedures for performing the improved MLCS technique are as follows.

1) Select the minimum (\min_p) and maximum percentage (\max_p) values. \min_p and \max_p values are used as percentage limits that must be met to determine the minimum and maximum intensity for each color component.

2) Calculate the $f_R(x, y)$ histogram, i.e., the red component.

3) Initialize the num_pixel_{left} and num_pixel_{right} variables with an initial value of 0. num_pixel_{left} is the total number of pixels starting from an intensity value of 0, while num_pixel_{right} is the total number of pixels starting from an intensity value of 255.

4) Initialize the $current_pixel$ variable with a value of 0.

5) Count num_pixel_{left} using Equation (1).

$$num_pixel_{left} = num_pixel_{left} + num_pix[current_pixel] \quad (1)$$

$num_pix[current_pixel]$ is the number of pixels at the intensity of $current_pixel$.

6) Check the probability of num_pixel_{left} using Equation (2), whether it satisfies the value of \min_p .

$$\frac{num_pixel_{left}}{Total\ number\ of\ pixels\ in\ the\ image} * 100 \geq \min_p \quad (2)$$

If the condition in Equation (2) is satisfied (true), set the minimum value of the red component (\min_R) equal to the value of the $current_pixel$ variable; else, set $current_pixel = current_pixel + 1$. Repeat steps 5) and 6) until the condition in Equation (2) is satisfied.

7) Initialize the $current_pixel$ variable with a value of 255.

8) Count num_pixel_{right} using Equation (3).

$$num_pixel_{right} = num_pixel_{right} + num_pix[current_pixel] \quad (3)$$

9) Check the probability of num_pixel_{right} using Equation (4), whether it satisfies the value of max_p .

$$\frac{num_pixel_{right}}{Total\ number\ of\ pixels\ in\ the\ image} * 100 \geq max_p \quad (4)$$

If the condition in Equation (4) is satisfied (true), set the maximum value of the red component (max_R) equal to the value of the $current_pixel$ variable; else, set $current_pixel = current_pixel - 1$. Repeat steps 8) and 9) until the condition in Equation (4) is satisfied.

10) Repeat steps 2)-9) to calculate the minimum and maximum values of the green and blue components (min_G , max_G , min_B , max_B).

11) Specify min_{RGB} and max_{RGB} values. min_{RGB} is obtained from the smallest min_R , min_G , and min_B values. max_{RGB} value is obtained from the largest max_R , max_G , and max_B values.

12) Calculate the new minimum and maximum values for the red component to reduce the dependence on local features using Equations (5) and (6). It is done to minimize color changes in the contrast-enhanced image.

$$new_min_R = \frac{min_R + min_{RGB}}{2} \quad (5)$$

$$new_max_R = \frac{max_R + max_{RGB}}{2} \quad (6)$$

13) Calculate the new minimum and maximum values for green and blue components (new_min_G , new_max_G , new_min_B , new_max_B) as in Equations (5) and (6).

14) Stretch the contrast of the pixels on the red component using linear contrast stretching (LCS) equation (7) [23].

$$out_R(x, y) = 255 * \left[\frac{(in_R(x, y) - new_min_R)}{new_max_R - new_min_R} \right] \quad (7)$$

$out_R(x, y)$ is the new pixel value, and $in_R(x, y)$ is the input pixel value at the (x, y) position.

15) Do the same for the green and blue components to produce $out_G(x, y)$ and $out_B(x, y)$ using Equation (7) with the input pixel values, new_min , and new_max of the green and blue components.

16) Combine $out_R(x, y)$, $out_G(x, y)$, and $out_B(x, y)$ to form a contrast-enhanced image.

In this study, the min_p and max_p values used in Equations (2) and (4) are 1%. These value are based on the previous experiment that tested three sets of min_p and max_p values: Set 1 is $min_p = 1\%$ and $max_p = 1\%$, Set 2 is $min_p = 1\%$ and $max_p = 10\%$, and Set 3 is $min_p = 0.5\%$ and $max_p = 10\%$ [19]. Set 1 uses a small percentage value of 1% to obtain a minimum and maximum pixel intensity different from the LCS method. Set 2 and 3 to measure the effect of stretching on the histogram pixels on the left and right sides. Based on the distribution separation measure, Set 1 gave the best results compared to Set 2 and Set 3.

Step 2: The proposed method is not only to increase the image contrast but also to preserve the color information of the processed image. In this step, the color preservation framework was used to improve the maintenance of color information using Equation (8) [22].

$$PRC_{IMG} = \delta(INT_{IMG}) + (1 - \delta)(INT_{IMG}) \quad (8)$$

INT_{IMG} is the contrast enhanced image generated from Step 1, INT_{IMG} is the raw malaria image, and PRC_{IMG} is the resulting color preservation image. The determination of the optimum gamma value is based on the following rules: 1) the range of the gamma value is $0 \leq \delta \leq 1$, 2) if $\delta = 0$, then $PRC_{IMG} = INP_{IMG}$ and this is a condition where maximum color preservation occurs without any contrast enhancing in the PRC_{IMG} , 3) if $\delta = 1$, then $PRC_{IMG} = INT_{IMG}$ and this is a condition where minimum color preservation occurs

with contrast enhancement in the PRC_{IMG} . The proposed method should provide better color preservation, so the choice of δ value should result in a lower AMBE measurement than the previous method. AMBE measurement is described in Section 3 of this paper.

3. Experiments. In this section, we demonstrate the performance of the proposed methods, namely improved MLCS (IMLCS) and IMLCS with color preserving framework (IMLCS-CPF), compared to previous linear-based contrast enhancement methods, like LCS and MLCS. This experiment used a public dataset from the Malaria Parasite Image Database (MP-IDB) for image processing and analysis [24]. The dataset has been acquired using a Leica DM2000 optical laboratory microscope at 100x magnification. The original image resolution of the dataset is 2592×1944 pixels. For testing the image enhancement method in this study, the Region of Interest (ROI) of Plasmodium was manually cropped with a resolution of 800×600 pixels. Figure 2 presents ROI images of Plasmodium malariae, falciparum, and vivax.

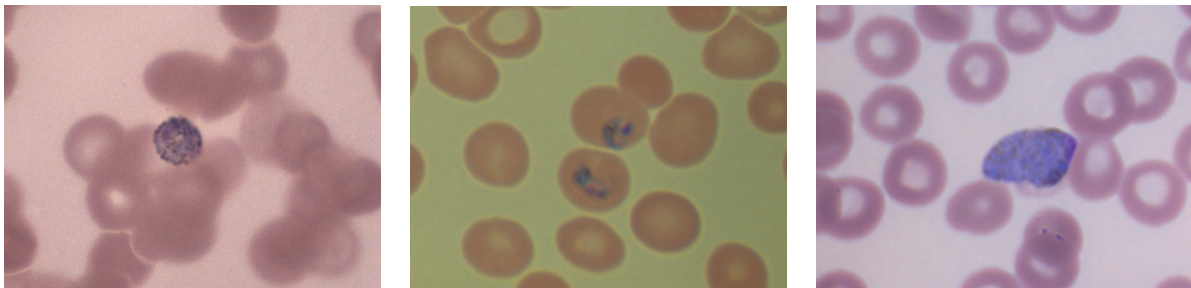


FIGURE 2. ROI Plasmodium malariae, falciparum, and vivax

Figure 3 shows enhancement results of various methods for Plasmodium malariae (left column), falciparum (middle column), and vivax (right column) images. The results of the LCS (a-c) and MLCS (d-f) methods can enhance the contrast image so that the appearance of Plasmodium and erythrocytes becomes clear. However, the LCS and MLCS methods resulted in color changes in Plasmodium and erythrocytes so that the information on the texture and structure of the original color could be changed. The results of the proposed IMLCS (g-i) and IMLCS-CPF methods (j-l) can enhance the contrast of the given image, but the IMLCS-CPF method is better at retaining color information.

Table 1 shows the measurement results of absolute mean brightness error (AMBE) and peak signal to noise ratio (PSNR) values for 12 Plasmodium images. AMBE is used to compute the difference in mean brightness between original and enhanced images. In the case of contrast enhancement, an image should retain its original brightness. The lower value of AMBE indicates good brightness preservation on the enhanced image. The AMBE value can be obtained using Equation (9) [25]. $E(I_r)$ and $E(I_e)$ are the mean brightness of the original and enhanced images, respectively.

$$AMBE = |E(I_r) - E(I_e)| \quad (9)$$

The PSNR value is used to measure image quality. The higher value means that the enhanced image has better image quality. Mathematical expression to compute PSNR between original and enhanced images is given in Equation (10) [25].

$$PSNR = 10 \log_{10} \frac{(L - 1)^2}{MSE} \quad (10)$$

L represents discrete gray levels, and in the case of an 8-bit image, $L - 1 = 255$. MSE is mean square error, calculated using Equation (11) [25]. $X(i, j)$ and $Y(i, j)$ represent pixel intensity values at location (i, j) in the original and enhanced images, respectively.

$$MSE = \frac{1}{MN} \sum_{i=1}^M \sum_{j=1}^N |X(i, j) - Y(i, j)|^2 \quad (11)$$

In Table 1, the IMLCS method produces a better AMBE average value than the LCS and MLCS. However, in Image₇, MLCS gives a better AMBE value than IMLCS. The IMLCS method combined with CPF can provide better AMBE values than the IMLCS, MLCS, and LCS methods in Image₇. Furthermore, we can see that the proposed IMLCS-CPF method has the smallest AMBE values in all 12 images. Based on Table 1, the

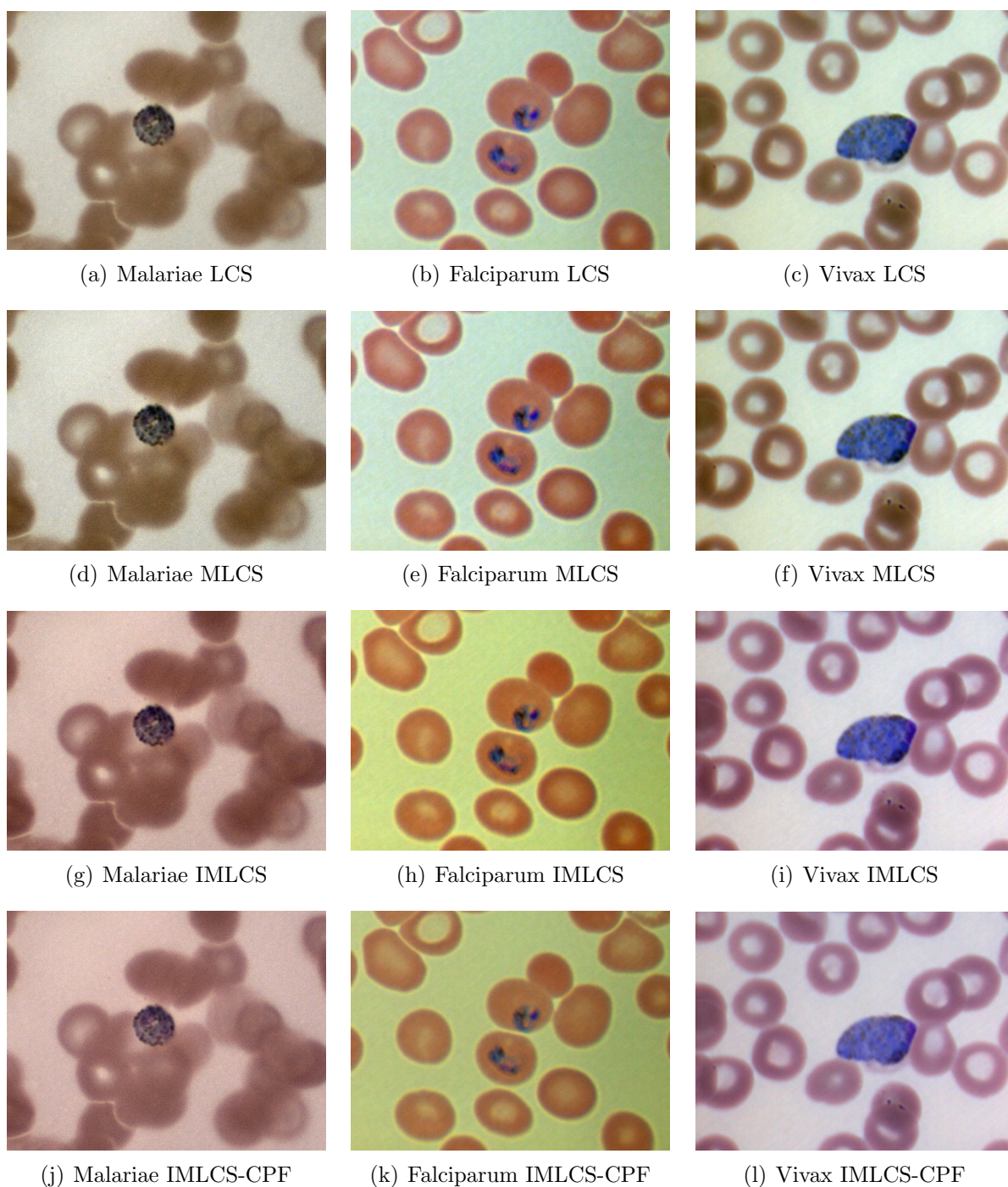


FIGURE 3. Enhancement results of *Plasmodium malariae*, *falciparum*, and *vivax* images using LCS, MLCS, IMLCS, and IMLCS-CPF methods. For these resulting images, we have considered $\min_p = 1\%$, $\max_p = 1\%$, and $\delta = 0.6$.

TABLE 1. AMBE and PSNR values for LCS, MLCS, IMLCS, IMLCS-CPF methods

Images	AMBE				PSNR			
	LCS	MLCS	IMLCS	IMLCS-CPF	LCS	MLCS	IMLCS	IMLCS-CPF
Image ₁	58.115	57.771	26.567	15.54	13.397	13.218	16.855	21.401
Image ₂	56.65	57.511	25.887	15.123	13.556	13.218	16.696	21.243
Image ₃	57.796	57.875	26.72	15.63	13.624	13.408	16.76	21.308
Image ₄	45.249	45.933	13.203	7.593	14.337	13.508	16.098	20.606
Image ₅	24.711	22.797	22.84	14.141	19.545	18.662	19.075	23.303
Image ₆	14.713	11.342	10.712	6.865	21.935	20.591	21.964	26.164
Image ₇	11.243	4.901	6.054	3.208	21.195	19.355	22.353	26.827
Image ₈	33.409	33.961	25.332	15.613	18.374	17.182	18.895	23.113
Image ₉	15.371	14.004	0.476	0.142	18.699	17.95	21.186	25.595
Image ₁₀	21.688	18.554	10.773	6.896	20.377	19.361	24.579	28.676
Image ₁₁	15.043	16.406	3.667	2.6	18.163	16.738	21.739	26.015
Image ₁₂	54.109	55.539	23.409	13.715	13.438	13.044	15.721	20.246
Average	34.008	33.050	16.303	9.756	17.22	16.353	19.327	23.708

proposed IMLCS-CPF method using $\delta = 0.6$ has the lowest average AMBE value among the other techniques, which means that the IMLCS-CPF can maintain the color information of the original image in the enhanced image. $\delta < 0.6$ will result in a smaller AMBE value, but the quality of the contrast enhancement will decrease. Meanwhile, $\delta > 0.6$ will reduce the color preservation ability. The PSNR value of the IMLCS-CPF method also gives the highest value. It indicates that the IMLCS-CPF method produces better contrast enhancement than the LCS, MLCS, and IMLCS methods. From the measurement results of AMBE and PSNR values, the proposed IMLCS-CPF method can produce a good contrast enhancement while preserving the color information of the original image. It has also been proven in the image resulting from the IMLCS-CPF method in Figures 3(j)-3(l). The appearance of the texture and morphology of the Plasmodium becomes clearer while maintaining the coloring structure from the original image so that the image resulting from the contrast enhancement looks natural.

4. Conclusions. We proposed an improved method to enhance the contrast of color malaria images while retaining the coloring structure of the original image. From the experimental results, the AMBE value of the proposed method is less compared to LCS, MLCS, and IMLCS methods. The proposed method also has a better PSNR value than the other methods. Based on the AMBE and PSNR values analysis, the proposed IMLCS-CPF method provides good contrast enhancement while preserving the color information of the original image. Hence, this method can clarify the appearance of Plasmodium and erythrocytes in the image of thin blood smears so that the enhanced images would become helpful in improving the performance of visual examination of malaria through a microscope or facilitate the segmentation process in an automatic malaria diagnosis system.

Acknowledgment. The authors would like to thank the Ministry of Research and Higher Education of the Republic of Indonesia through Universitas Gadjah Mada, which has funded this research with contract numbers: 1894/UN1/DITLIT/Dit-Lit/PT.01.03/2022.

REFERENCES

- [1] J. Hawadak, R. R. D. Nana and V. Singh, Global trend of Plasmodium malariae and Plasmodium ovale spp. malaria infections in the last two decades (2000-2020): A systematic review and meta-analysis, *Parasites and Vectors*, vol.14, no.1, pp.1-14, 2021.
- [2] M. Poostchi, K. Silamut, R. J. Maude, S. Jaeger and G. Thoma, Image analysis and machine learning for detecting malaria, *Translational Research*, vol.194, pp.36-55, 2018.
- [3] Global Malaria Programme WHO, *World Malaria Report 2021*, World Health Organization, 2021.
- [4] A. Loddo, C. di Ruberto and M. Kocher, Recent advances of malaria parasites detection systems based on mathematical morphology, *Sensors*, vol.18, no.2, 513, 2018.
- [5] N. Tangpukdee, C. Duangdee, P. Wilairatana and S. Krudsood, Malaria diagnosis: A brief review, *The Korean Journal of Parasitology*, vol.47, no.2, pp.93-102, 2009.
- [6] F. B. Tek, A. G. Dempster and I. Kale, Computer vision for microscopy diagnosis of malaria, *Malaria Journal*, vol.8, no.1, pp.1-14, 2009.
- [7] Z. Jan, A. Khan, M. Sajjad, K. Muhammad, S. Rho and I. Mehmood, A review on automated diagnosis of malaria parasite in microscopic blood smears images, *Multimed. Tools Appl.*, vol.77, no.8, pp.9801-9826, 2018.
- [8] J. Somasekar, G. Ramesh, G. Ramu, P. D. K. Reddy, B. E. Reddy and C. H. Lai, A dataset for automatic contrast enhancement of microscopic malaria infected blood RGB images, *Data in Brief*, vol.27, 104643, 2019.
- [9] A. N. N. Afifah, Indrabayu, A. Suyuti and Syafaruddin, A review on image processing techniques for damage detection on photovoltaic panels, *ICIC Express Letters*, vol.15, no.7, pp.779-790, 2021.
- [10] Y. Purwar, S. L. Shah, G. Clarke, A. Almgairi and A. Muehlenbachs, Automated and unsupervised detection of malarial parasites in microscopic images, *Malaria Journal*, vol.10, no.1, pp.1-11, 2011.
- [11] J. Somasekar and B. E. Reddy, Segmentation of erythrocytes infected with malaria parasites for the diagnosis using microscopy imaging, *Computers & Electrical Engineering*, vol.45, pp.336-351, 2015.
- [12] J. D. Chaya and R. N. Usha, Predictive analysis by ensemble classifier with machine learning models, *International Journal of Computers and Applications*, pp.1-8, 2019.
- [13] S. N. A. M. Kanafiah, M. Y. Mashor, W. A. Mustafa, Z. Mohamed, S. A. A. Shukor, H. Yazid and Z. R. Yahya, A novel contrast enhancement technique based on combination of local and global statistical data on malaria images, *Journal of Biomimetics, Biomaterials and Biomedical Engineering*, vol.38, pp.23-30, 2018.
- [14] W. A. Mustafa and H. Yazid, Image enhancement technique on contrast variation: A comprehensive review, *Journal of Telecommunication, Electronic and Computer Engineering*, vol.9, no.3, pp.199-204, 2017.
- [15] H. A. Nugroho, A. Darajatun, I. Ardiyanto and R. L. B. Buana, Classification of Plasmodium malariae dan Plasmodium ovale in microscopic thin blood smear digital images, *International Journal on Advanced Science, Engineering and Information Technology*, vol.8, no.6, pp.2301-2307, 2018.
- [16] A. Molina, S. Alférez, L. Boldú, A. Acevedo, J. Rodellar and A. Merino, Sequential classification system for recognition of malaria infection using peripheral blood cell images, *Journal of Clinical Pathology*, vol.73, no.10, pp.665-670, 2020.
- [17] A. S. Abdul-Nasir, M. Y. Mashor and Z. Mohamed, Segmentation of malaria parasite based on stained blood cells detection, *Journal of Biomimetics, Biomaterials and Biomedical Engineering*, vol.24, pp.43-55, 2015.
- [18] A. S. Abdul-Nasir, M. Y. Mashor and Z. Mohamed, Clustering approach for unsupervised segmentation of malarial Plasmodium vivax parasite, *AIP Conference Proceedings*, 020004, 2017.
- [19] A. S. Abdul-Nasir, M. Y. Mashor and Z. Mohamed, Modified global and modified linear contrast stretching algorithms: New colour contrast enhancement techniques for microscopic analysis of malaria slide images, *Computational and Mathematical Methods in Medicine*, vol.2012, pp.1-16, 2012.
- [20] H. A. Nugroho, M. S. Wibawa, N. A. Setiawan, E. E. H. Murhandarwati and R. L. B. Buana, Identification of Plasmodium falciparum and Plasmodium vivax on digital image of thin blood films, *Indonesian Journal of Electrical Engineering and Computer Science*, vol.13, no.3, pp.933-944, 2019.
- [21] S. N. A. M. Kanafiah, M. Y. Mashor, Z. Mohamed, Y. C. Way, S. A. A. Shukor and Y. Jusman, An intelligent classification system for trophozoite stages in malaria species, *Intelligent Automation and Soft Computing*, vol.34, no.1, pp.687-697, 2022.
- [22] B. Gupta and M. Tiwari, Minimum mean brightness error contrast enhancement of color images using adaptive gamma correction with color preserving framework, *Optik*, vol.127, no.4, pp.1671-1676, 2016.
- [23] U. K. Ngah, T. H. Ooi, N. E. A. Khalid and P. A. Venkatachalam, The seed based region growing image processing with embedded enhancement techniques, *Proc. of the 2nd International Conference on Computers in Industry (ICCI'00)*, 2000.

- [24] A. Loddo, C. Di Ruberto, M. Kocher and G. Prod'Hom, MP-IDB: The malaria parasite image database for image processing and analysis, *Sipaim-Miccai Biomedical Workshop*, pp.57-65, 2018.
- [25] M. A. Qureshi, A. Beghdadi and M. Deriche, Towards the design of a consistent image contrast enhancement evaluation measure, *Signal Processing: Image Communication*, vol.58, pp.212-227, 2017.